

Received July 28, 2021, accepted August 16, 2021, date of publication September 6, 2021, date of current version September 21, 2021.

Digital Object Identifier 10.1109/ACCESS.2021.3110597

The Harmonically Coupled Admittance Matrix of the Single-Phase Diode Rectifier

LUIS F. BEITES¹, JULIO G. MAYORDOMO¹,
AND XAVIER YANG², (Senior Member, IEEE)

¹Universidad Politécnica de Madrid, 28040 Madrid, Spain

²Power Distribution Department, Electricité de France (EDF) R&D, 91120 Palaiseau, France

Corresponding author: Luis F. Beites (lbeites@etsii.upm.es)

ABSTRACT The convergence of the iterative harmonic analysis (IHA) of networks with nonlinear loads can be improved if the Gauss algorithm is replaced by the modular decoupled Newton solution (M-DNS). The core of the M-DNS is the harmonically coupled admittance matrix (HCAM) of each nonlinear load. HCAM of high-power converters has received special attention. However, the HCAM of single-phase uncontrolled rectifiers (SPUR) with capacitive smoothing has only been developed under certain simplifications for the SPUR. A reference model for the SPUR is extensively accepted and a detailed analytical procedure (DAP) is the fastest way to obtain the steady state of the SPUR. The main object of this paper is to present a HCAM for the reference model of SPUR with capacitive smoothing. This HCAM is directly derived from a DAP for the converter. Convergence properties of the IHA with this HCAM are studied.

INDEX TERMS Discontinuous conduction mode (DCM), uncontrolled rectifiers, harmonics, operating point setting.

I. INTRODUCTION

It is widely accepted that a reference model for the SPUR with capacitive dc smoothing is formed by a R-L ac branch, a R-C dc branch, and an ideal diode bridge. Assuming that the ac terminal voltage is known, the steady state solution of the reference model (converter solution) can be efficiently achieved by using detailed analytical procedures (DAP) [1]–[6]. Two nonlinear equations are enough to estimate the switching instants with these DAPs. After that, a very fast harmonic analysis is possible by using analytical expressions for the ac harmonic currents. A good agreement between measurement and simulation is achieved with the reference model [6].

The integration of the reference model into the ac network has been carried out in [3], and the IHA is performed by means of the Gauss Algorithm within a frequency domain formulation. The IHA involves to update the terminal harmonic voltages in the iterative process. The modular decoupled Newton solution (M-DNS), described in [7] for high powered converters, provides better convergence than the Gauss Algorithm. The core of the M-DNS is the HCAM of the

converter [8]–[9]. The HCAM of the SPUR has been recently proposed assuming certain simplifications. First, infinite capacitance and a pure inductive ac branch are assumed in [11]. Also, other previous works [10], [12] represent compact fluorescent lamps (CLFs) by means of SPUR models where the ac branch is omitted [10] or the inductance of the ac branch is not considered [12]. In spite of that, good results are obtained in [12] for reproducing the “poor-average CLF harmonic spectra category”. The corresponding HCAMs are derived in [10] and [12]. The HCAM of the reference model presents a more complex form.

A frequency domain formulation is used in [3] and in this paper. As was stated in [10] for CFLs “the main advantage of a frequency domain formulation is that the reference model for SPURs can be included in harmonic power flow programs for large scale SPUR penetration studies. Such studies are very difficult to do by using the EMTP-type domain simulations”. The main object of this paper is to develop the HCAM for the reference model. This task is relatively easy if the reference model is represented by a DAP and the phasor associated with the transient component of the conduction interval is eliminated by a similar method as used in [13]. The resulting HCAM is integrated in the M-DNS to solve the convergence problems of the IHA when the Gauss algorithm

The associate editor coordinating the review of this manuscript and approving it for publication was Zhixiang Zou¹.

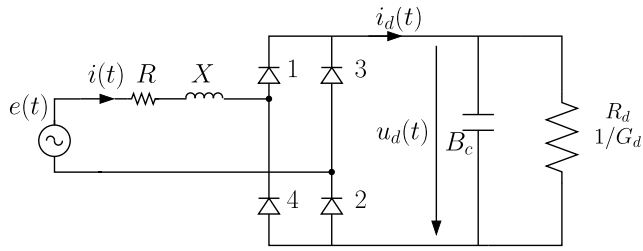


FIGURE 1. Basic scheme for the analysis.

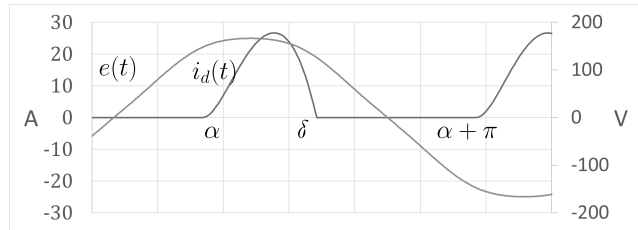


FIGURE 2. Basic subinterval for the analysis.

is used. Moreover, a merit figure is proposed to treat the converter operating point in terms of power. The resulting DAP for the converter solution uses a full Newton formulation in which the switching instants and the dc resistance are treated as unknowns and the terms of the Jacobian matrix are evaluated from analytical expressions.

II. CONVERTER SOLUTION

The scheme of figure 1 is the system to be studied. The notation of [13] is also here used. Hence, reactance X and susceptance B_c are parameters at the fundamental frequency, ω_1 is the fundamental angular frequency (100π or 120π rad/s) and τ is an angle defined as $\tau = \omega_1 t$, where t is a time instant. Hence, the ac and dc instantaneous voltages and currents are functions of angle τ , and they are expressed by:

$$e = \sum_{m=1}^{n_h} \text{Im}\{\hat{E}_m \cdot e^{jm\tau}\}; \quad i = \sum_{m=1}^{\infty} \text{Im}\{\hat{I}_m \cdot e^{jm\tau}\} \quad (1)$$

$$u_d = \sum_{k=0}^{\infty} \text{Im}\{\hat{U}_{dk} \cdot e^{jk\tau}\}; \quad i_d = \sum_{k=0}^{\infty} \text{Im}\{\hat{I}_{dk} \cdot e^{jk\tau}\} \quad (2)$$

Subscripts m and k are integers which indicate the order of a generic harmonic, and n_h is the order of the harmonic of highest frequency to be considered on ac voltage $e(\tau)$. According to (2), dc components of dc magnitudes are related to the harmonic phasors by:

$$\hat{U}_{d0} = jU_d; \quad \hat{I}_{d0} = jI_d \quad (3)$$

Half-wave symmetry is assumed for voltage $e(\tau)$. Hence, ac magnitudes $e(\tau)$ and $i(\tau)$ only present odd harmonics while dc magnitudes $u_d(\tau)$ and $i_d(\tau)$ only contain even harmonics and dc components. Only the positive half-wave of current $i(\tau)$ is needed for the analysis. This half-wave (or interval) is denoted by s , and it can be divided in a conduction

subinterval s_x and a discontinuity subinterval s_y . The limits of these intervals are described by the following basic angles (figure 2):

$$s = [\alpha, \alpha + \pi]; \quad s_x = [\alpha, \delta]; \quad s_y = [\delta, \alpha + \pi] \quad (4)$$

DC current $i_d(\tau)$ exhibits a discontinuous behaviour in subinterval s_y . This condition is given by:

$$i_d(\tau) = 0 \quad \forall \tau \in s_y \quad (5)$$

while current $i_d(\tau)$ is equal to zero in the limits of subinterval s_x , namely:

$$i_d(\alpha) = i_d(\delta) = 0 \quad (6)$$

The converter solution involves the calculation of basic angles α and δ when ac voltage $e(\tau)$ and parameters R, X, B_c, G_d are known. With this, the dc and ac harmonic components are completely defined.

A. CONDUCTION SUBINTERVAL

Diodes 1 and 2 are in conduction in subinterval s_x . Hence, dc magnitudes u_d and i_d in subinterval s_x are related by the following two equations:

$$e = u_d + R \cdot i_d + X \cdot i'_d \quad (7)$$

$$i_d = G_d \cdot u_d + B_c \cdot u'_d = B_c [\sigma \cdot u_d + u'_d]; \quad \sigma = G_d/B_c \quad (8)$$

where $i'_d = di_d(\tau)/d\tau$ and $u'_d = du_d(\tau)/d\tau$. The elimination of current i_d among (7) and (8) leads to the following differential equation of second order for voltage u_d :

$$u''_d + 2\xi u'_d + k_o^2 u_d = f(\tau) \quad \text{for } \tau \in s_x \quad (9)$$

$$2\xi = \frac{R}{X} + \frac{G_d}{B_c}; \quad k_o^2 = \frac{RG_d + 1}{XB_c}; \quad f(\tau) = \frac{e(\tau)}{XB_c} \quad (10)$$

The solution of (9) presents a steady state component u_s and a transient component u_t , so that:

$$u_d = u_s + u_t \quad \text{for } \tau \in s_x \quad (11)$$

Voltage u_s is obtained from:

$$u_s = \sum_{m=1}^{n_h} \text{Im}\{\hat{U}_{s,m} \cdot e^{jm\tau}\}; \quad \hat{U}_{s,m} = c_m \cdot \hat{E}_m \quad (12)$$

$$c_m = 1/[1 + (R + jmX)(G_d + jmB_c)] \quad (13)$$

Voltage u_t presents the following form when $\xi < k_o$:

$$u_t = \text{Im}\{\hat{U}_t \cdot e^{\underline{\nu}\tau}\}; \quad k_n = \sqrt{k_o^2 - \xi^2}; \quad \underline{\nu} = -\xi + jk_n \quad (14)$$

The derivatives of components u_s and u_t are given by:

$$u'_s = \sum_{m=0}^{n_h} \text{Im}\{\hat{U}'_{s,m} \cdot e^{jm\tau}\}; \quad \hat{U}'_{s,m} = jm \cdot c_m \cdot \hat{E}_m \quad (15)$$

$$u'_t = \text{Im}\{\hat{U}'_t \cdot e^{\underline{\nu}\tau}\}; \quad \hat{U}'_t = \underline{\nu} \cdot \hat{U}_t \quad (16)$$

The steady state component is completely determined by (12) and (13). However, phasor \hat{U}_t of the transient component is not known in advance, and its value is obtained from the basic angles provided by the converter solution indicated

in appendix A. Once the basic angles are known, phasor \hat{U}_t is estimated from (72) and (77), so that:

$$\hat{U}_t = \frac{1}{k_n}(a_2 - \underline{v}^* a_1) \cdot \varepsilon^{-\underline{v}\alpha} \quad (17)$$

where the terms a_1 and a_2 are indicated in (68) and (69) and they can also be expressed by:

$$j2a_1 = \sum_{m=1}^{n_h} (\underline{h}_{1m} \cdot \hat{E}_m \cdot \varepsilon^{jm\alpha} - \underline{h}_{1m}^* \cdot \hat{E}_m^* \cdot \varepsilon^{-jm\alpha}) \quad (18)$$

$$j2a_2 = \sum_{m=1}^{n_h} (\underline{h}_{2m} \cdot \hat{E}_m \cdot \varepsilon^{jm\alpha} - \underline{h}_{2m}^* \cdot \hat{E}_m^* \cdot \varepsilon^{-jm\alpha}) \quad (19)$$

$$\underline{h}_{1m} = 1 - \underline{c}_m; \quad \underline{h}_{2m} = -(\sigma + jm\underline{c}_m) \quad (20)$$

To perform harmonic analysis, the voltages u_s and u_t of (12) and (14) can also be expressed by:

$$u_t(\tau) = \frac{1}{j2} (\hat{U}_t \varepsilon^{j\tau} - \hat{U}_t^* \varepsilon^{-j\tau}) \quad (21)$$

$$u_s(\tau) = \frac{1}{j2} \sum_{m=1}^{n_h} (\underline{c}_m \cdot \hat{E}_m \varepsilon^{jm\tau} - \underline{c}_m^* \cdot \hat{E}_m^* \varepsilon^{-jm\tau}) \quad (22)$$

III. DC AND AC HARMONICS

Due to the symmetry properties, the harmonic analysis involves to estimate the complex function \underline{F}_k :

$$\underline{F}_k(i_d) = \frac{j2}{\pi \cdot \rho_k} \int_{\alpha}^{\delta} i_d \cdot \varepsilon^{-jk\tau} d\tau; \quad \rho_k = \begin{cases} 1 & \text{for } k \neq 0 \\ 2 & \text{for } k = 0 \end{cases} \quad (23)$$

With this, the ac harmonic current \hat{I}_k , and the dc harmonic current \hat{I}_{dk} are obtained from the following scheme:

$$\begin{aligned} \hat{I}_k &= \underline{F}_k(i_d) & \text{for } k = 1, 3, 5, \dots \\ \hat{I}_{dk} &= \underline{F}_k(i_d) & \text{for } k = 0, 2, 4, \dots \end{aligned} \quad (24)$$

In accordance with the developments of appendix B, function \underline{F}_k presents the following compact form:

$$\underline{F}_k = \underline{Y}_{k,t}^{(1)} \hat{U}_t + \underline{Y}_{k,t}^{(2)} \hat{U}_t^* + \sum_{m=1}^{n_h} (\underline{Y}_{km,s}^{(1)} \hat{E}_m + \underline{Y}_{km,s}^{(2)} \hat{E}_m^*) \quad (25)$$

where:

$$\underline{d}_t = G_d + \underline{v}B_c \quad \underline{d}_m = \underline{c}_m(G_d + jm \cdot B_c) \quad (26)$$

$$\underline{Y}_{k,t}^{(1)} = \underline{d}_t \cdot \underline{\beta}_{k,t}^{(1)}; \quad \underline{\beta}_{k,t}^{(1)} = \frac{\varepsilon^{(\underline{v}-jk)\delta} - \varepsilon^{(\underline{v}-jk)\alpha}}{\pi \rho_k (\underline{v} - jk)} \quad (27)$$

$$\underline{Y}_{k,t}^{(2)} = \underline{d}_t^* \cdot \underline{\beta}_{k,t}^{(2)}; \quad \underline{\beta}_{k,t}^{(2)} = -\frac{\varepsilon^{(\underline{v}^*-jk)\delta} - \varepsilon^{(\underline{v}^*-jk)\alpha}}{\pi \rho_k (\underline{v}^* - jk)} \quad (28)$$

$$\underline{Y}_{km,s}^{(1)} = \underline{d}_m \cdot \underline{\beta}_{km,s}^{(1)}; \quad \underline{\beta}_{km,s}^{(1)} = j \frac{\varepsilon^{-j(k-m)\delta} - \varepsilon^{-j(k-m)\alpha}}{\pi \rho_k (k - m)} \quad (29)$$

$$\underline{Y}_{km,s}^{(2)} = \underline{d}_m^* \cdot \underline{\beta}_{km,s}^{(2)}; \quad \underline{\beta}_{km,s}^{(2)} = -j \frac{\varepsilon^{-j(k+m)\delta} - \varepsilon^{-j(k+m)\alpha}}{\pi \rho_k (k + m)} \quad (30)$$

When $m = k$ in the calculation of ac current \hat{I}_k , term $\underline{\beta}_{kk,s}^{(1)} = (\delta - \alpha)/\pi$. It is important to note that function \underline{F}_k

of (25) provides ac harmonic currents if k is an odd integer or dc harmonic currents if k is an even integer. Integer m is always an odd integer. Once the dc harmonic current \hat{I}_{dk} is evaluated from (25), dc harmonic voltage \hat{U}_{dk} is obtained from:

$$\hat{U}_{dk} = \frac{\hat{I}_{dk}}{G_d + jkB_c} \quad (31)$$

The dc components I_d and U_d are derived from (3), (25) and (31) when $k = 0$.

IV. HARMONICALLY COUPLED ADMITTANCE MATRIX

The construction of the Harmonically Coupled Admittance Matrix (HCAM) requires to express phasor \hat{U}_t in function of ac voltage phasors \hat{E}_m . To do that, terms a_1 and a_2 of (18) and (19) are introduced in (17). After several developments, and taking into account (20), phasor \hat{U}_t is equivalent to:

$$\hat{U}_t = \sum_{m=1}^{n_h} (\underline{\mu}_{1m} \cdot \hat{E}_m + \underline{\mu}_{2m} \cdot \hat{E}_m^*) \quad (32)$$

$$\underline{\mu}_{1m} = j \frac{\sigma + \underline{v}^* - (\underline{v}^* - jm) \cdot \underline{c}_m}{2k_n} \cdot \varepsilon^{-(\underline{v}-jm)\alpha} \quad (33)$$

$$\underline{\mu}_{2m} = -j \frac{\sigma + \underline{v}^* - (\underline{v}^* + jm) \cdot \underline{c}_m^*}{2k_n} \cdot \varepsilon^{-(\underline{v}+jm)\alpha} \quad (34)$$

The elimination of \hat{U}_t between (25) and (32) leads to:

$$\underline{F}_k = \sum_{m=1}^{n_h} (\underline{Y}_{km}^{(1)} \cdot \hat{E}_m + \underline{Y}_{km}^{(2)} \cdot \hat{E}_m^*) \quad (35)$$

$$\underline{Y}_{km}^{(1)} = \underline{Y}_{km,s}^{(1)} + \underline{\mu}_{1m} \cdot \underline{Y}_{k,t}^{(1)} + \underline{\mu}_{2m}^* \cdot \underline{Y}_{k,t}^{(2)} \quad (36)$$

$$\underline{Y}_{km}^{(2)} = \underline{Y}_{km,s}^{(2)} + \underline{\mu}_{2m} \cdot \underline{Y}_{k,t}^{(1)} + \underline{\mu}_{1m}^* \cdot \underline{Y}_{k,t}^{(2)} \quad (37)$$

It is evident from (23) and (35) that ac and dc harmonic currents can be directly obtained from the ac harmonic voltages \hat{E}_m . When the term k is an odd integer, $\underline{F}_k = \hat{I}_k$, and $\underline{Y}_{km}^{(1)}$ and $\underline{Y}_{km}^{(2)}$ are the complex admittances of the HCAM. The real and imaginary parts of the HCAM are obtained as in [7] by:

$$\begin{aligned} G_{km}^{(+)} &= \text{Re} \left\{ \underline{Y}_{km}^{(1)} + \underline{Y}_{km}^{(2)} \right\} & G_{km}^{(-)} &= \text{Re} \left\{ \underline{Y}_{km}^{(1)} - \underline{Y}_{km}^{(2)} \right\} \\ B_{km}^{(+)} &= \text{Im} \left\{ \underline{Y}_{km}^{(1)} + \underline{Y}_{km}^{(2)} \right\} & B_{km}^{(-)} &= \text{Im} \left\{ \underline{Y}_{km}^{(2)} - \underline{Y}_{km}^{(1)} \right\} \end{aligned} \quad (38)$$

Hence, (35) can be expressed by:

$$\begin{bmatrix} \hat{I}_k^{(r)} \\ \hat{I}_k^{(x)} \end{bmatrix}_{n\ell} = \sum_{m=1}^{n_h} \begin{bmatrix} G_{km}^{(+)} & B_{km}^{(-)} \\ B_{km}^{(+)} & G_{km}^{(-)} \end{bmatrix}_{n\ell} \cdot \begin{bmatrix} \hat{E}_m^{(r)} \\ \hat{E}_m^{(x)} \end{bmatrix} \quad (39)$$

where:

$$\begin{aligned} \hat{I}_k^{(r)} &= \text{Re} \left\{ \hat{I}_k \right\}; & \hat{E}_k^{(r)} &= \text{Re} \left\{ \hat{E}_k \right\} \\ \hat{I}_k^{(x)} &= \text{Im} \left\{ \hat{I}_k \right\}; & \hat{E}_k^{(x)} &= \text{Im} \left\{ \hat{E}_k \right\} \end{aligned} \quad (40)$$

The HCAM is the core of the modular decoupled Newton solution (M-DNS) described in [7]. In the M-DNS, the relation of (39) is written in a compact form by:

$$(I)_{n\ell} = (Y)_{n\ell} \cdot (E) \quad (41)$$

$(I)_{n\ell}$ and (E) are column vectors of $2n_h$ elements, and $(Y)_{n\ell}$, or HCAM, is a square matrix of $2n_h$ columns. The external part of the converter (the ac network) is assumed linear, and according to [7] it can be represented by:

$$(I)_{\ell} = (I_g)_{\ell} - (Y)_{\ell} \cdot (E) \quad (42)$$

The M-DNS involves to solve two partial iterative processes (PIP): the converter solution (PIP1) described in appendix A and the ac network solution (PIP2) in which the vector of the terminal harmonic voltages is updated to a new value $(E)^{new}$. Taking into account (41), (42) of this paper and (22) in [7], this algorithm is expressed by:

$$(I_g)_{\ell} = [(Y)_{\ell} + (Y)_{n\ell}] \cdot (E)^{new} \quad (43)$$

The relation (43) is equivalent to a set of $2n_h$ equations which are solved by means of the conventional methods for linear systems. With this, the unknowns, contained in the vector $(E)^{new}$, are calculated. The elements of the vector $(I_g)_{\ell}$ and of matrix $(Y)_{\ell}$ are not modified in the whole iterative process (WIP). The specific steps of the WIP are:

- Step 1: set initial values for variables (E) , α and δ . They are selected according to the ideal rectifier with sinusoidal AC voltages [14]. Make $iter = 0$.
- Step 2: the converter solution (PIP1) is obtained by solving equations (79) and (80) until the convergence is reached with a tolerance ϵ_I . The PIP1 involves to perform several iterations by means of the Newton method. Updated values of angles α and δ are provided for the next steps.
- Step 3: calculate $(Y)_{n\ell}$ of the rectifier using angles α and δ evaluated in step 2. With this, the harmonic voltages of (E) are obtained from (43).
- Step 4: go to step 6 if the discrepancies of vector (E) among two consecutive iterations are less than a tolerance ϵ_{II} .
- Step 5: go to step 2 and make $iter = iter + 1$.
- Step 6: Print the results.

An alternative approach to the M-DNS is the Gauss algorithm (GA). The GA presents a modular and easy formulation and it has been proposed in several previous works. In accordance with the notation of this paper, the GA involves to solve the following set of equations for the PIP2:

$$(I_g)_{\ell} - (I)_{n\ell} = (Y)_{\ell} \cdot (E)^{new} \quad (44)$$

Matrix $(Y)_{\ell}$ do not present coupling among harmonic frequencies. Hence, each harmonic voltage can be individually updated, namely, a matrix formulation, as used in (43), is not required in this case, and the elements of vector $(I)_{n\ell}$ can be evaluated from (24) and (25). Although only one busbar with one converter is considered in this paper, the extension to distributed converters [7], connected at different busbars of the ac network, is straightforward for the M-DNS and for the GA.

The analytical expressions of the HCAM have been derived in this section for the reference model once the basic angles

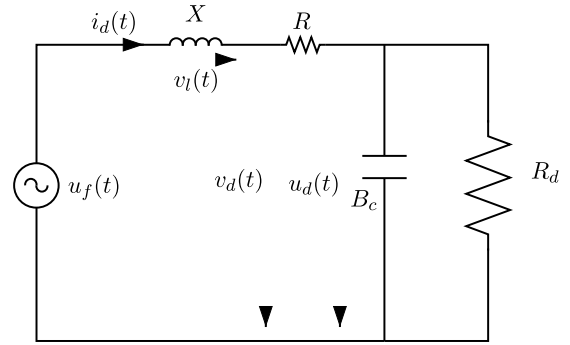


FIGURE 3. Basic scheme for the analysis.

are calculated from the converter solution provided by the DAP. Other DAPs, such as described in [6], provide the same results for these basic angles. Hence, the HCAM presented in this paper can be combined with the converter solution proposed in [6] to obtain a M-DNS with better convergence than the Gauss algorithm.

V. OPERATING POINT IN TERMS OF POWER

Until now, it is assumed in the analysis that the dc load is defined by a constant or specified conductance G_d . However, the dc load behaves as a constant power in many applications. In this case, the conductance G_d must be treated as a variable and an additional mismatch equation ΔF_c must be included in the system formed by ΔF_a and ΔF_b indicated in (79) and (80). Term ΔF_c is defined as:

$$\Delta F_c = P - P_{sp}; \quad P = G_d \cdot U_d^2 = I_d^2 / G_d \quad (45)$$

where P_{sp} is the specified power and P is the calculated power from the dc magnitudes U_d or I_d . Terms U_d and I_d , and therefore P , depend on variables α , δ and G_d . An analytical expression of $P(\alpha, \delta, G_d)$ is needed if a simultaneous updating of these variables is required in a full Newton formulation to obtain the fastest results for the converter solution. The sequential updating of [1] is a less robust and less efficient approach. An analytical expression of $I_d(\alpha, \delta, G_d)$ is directly obtained from (35) making $k = 0$, namely, $jI_d(\alpha, \delta, G_d) = \underline{F}_0$. However, admittances $Y_{0m}^{(1)}$ and $Y_{0m}^{(2)}$ present certain complexity. A more simple expression for $U_d(\alpha, \delta, G_d)$ is proposed in this paper which is derived from the scheme of figure 3 (dc side equivalent circuit) in which voltages u_f , v_l and v_d are related by:

$$\begin{aligned} u_f(\tau) &= v_l(\tau) + v_d(\tau) = e(\tau) \quad \forall \tau \in s_x(a) \\ u_f(\tau) &= v_d(\tau) = u_d(\tau) \quad \forall \tau \in s_y(b) \end{aligned} \quad (46)$$

The dc component V_d of voltage $v_d(\tau)$ is obtained from:

$$V_d = \frac{1}{\pi} \int_{\alpha}^{\alpha+\pi} v_d \cdot d\tau \quad (47)$$

Voltage V_d and its derivatives with respect to terms α , δ and G_d can be calculated from voltage $e(\tau)$, defined in (1),

and from functions $\bar{e}(\tau)$ and $e'(\tau)$:

$$\bar{e}(\tau) = \sum_{m=1}^{n_h} \text{Im}\{\hat{E}_m \cdot \frac{\varepsilon^{jm\tau}}{jm}\}; \quad e'(\tau) = \sum_{m=1}^{n_h} \text{Im}\{jm\hat{E}_m \cdot \varepsilon^{jm\tau}\} \quad (48)$$

The integral of voltage $v_\ell(\tau)$ is zero in subinterval s_x since $i_d(\alpha) = i_d(\delta) = 0$. On the other hand, $v_d(\tau) = u_d(\tau)$ in subinterval s_y . With these two properties, and considering (1), (48) and (63), voltage V_d is equivalent to:

$$V_d = \frac{\bar{e}(\delta) - \bar{e}(\alpha)}{\pi} + \frac{\varepsilon^{\sigma(\alpha+\pi-\delta)} - 1}{\pi\sigma} e(\alpha) \quad (49)$$

and their derivatives are given by:

$$\frac{\partial V_d}{\partial \alpha} = \frac{[\sigma e(\alpha) + e'(\alpha)]\varepsilon^{\sigma(\alpha+\pi-\delta)} - e'(\alpha) - \sigma e(\alpha)}{\pi\sigma} \quad (50)$$

$$\frac{\partial V_d}{\partial \delta} = \frac{e(\delta) - e(\alpha) \cdot \varepsilon^{\sigma(\alpha+\pi-\delta)}}{\pi} \quad (51)$$

$$\frac{\partial V_d}{\partial G_d} = \frac{e(\alpha) \cdot (\alpha + \pi - \delta) \cdot \varepsilon^{\sigma(\alpha+\pi-\delta)}}{\pi B_c \sigma^2} \quad (52)$$

On the other hand, the dc components are related by:

$$V_d = U_d + R \cdot I_d = (1 + R \cdot G_d) \cdot U_d \quad (53)$$

Therefore, the analytical expression for the calculated power is given by:

$$P(\alpha, \delta, G_d) = \frac{G_d}{(1 + R \cdot G_d)^2} V_d^2(\alpha, \delta, G_d) \quad (54)$$

where $V_d(\alpha, \delta, G_d)$ is estimated from (49). That is a merit figure for obtaining analytical expressions for the terms of the jacobian matrix:

$$\frac{\partial \Delta F_c}{\partial \alpha} = \frac{2G_d \cdot V_d}{(1 + R \cdot G_d)^2} \frac{\partial V_d}{\partial \alpha}; \quad \frac{\partial \Delta F_c}{\partial \delta} = \frac{2G_d \cdot V_d}{(1 + R \cdot G_d)^2} \frac{\partial V_d}{\partial \delta} \quad (55)$$

$$\frac{\partial \Delta F_c}{\partial G_d} = \frac{1 - R \cdot G_d}{(1 + R \cdot G_d)^3} V_d^2 + \frac{2G_d \cdot V_d}{(1 + R \cdot G_d)^2} \frac{\partial V_d}{\partial G_d} \quad (56)$$

The expressions for terms $\partial \Delta F_a / \partial G_d$ and $\partial \Delta F_b / \partial G_d$ are indicated in appendix C.

VI. TEST 1 FOR A SINGLE-PHASE RECTIFIER

This test is proposed in Fig 5 in [1], where a set of 10 identical 100 W rectifiers share a common system impedance $\underline{Z} = 0,4 + j0,25 \Omega$. Each unit has a dc capacitor of 370 μF . That leads to an equivalent rectifier of 1000 W with a dc capacitor of 3.7 mF. The equivalent rectifier is connected to a system of 120 V, 60 Hz. Impedance \underline{Z} provides in this case the internal parameters R and X for the converter solution, so that: $R = 0,4 \Omega$ and $X = 0,25 \Omega$. A fundamental voltage of $\hat{E}_1 = 120\sqrt{2} \cdot \exp(j0)$ is considered in test 1a while and a fifth harmonic voltage of $\hat{E}_5 = 0,02 \times 120\sqrt{2} \cdot \exp(j180^\circ)$ is added for test 1b. The load is defined in both cases by a specified power of 1000 W. Test 1a and test 1b require to perform the converter solution with fixed values for the aforementioned terminal harmonic voltages \hat{E}_k .

The basic angles and the dc resistance converge in very few iterations as shown in Table 1. It is due to the fact

TABLE 1. Convergence properties for Test 1.

iter	Test 1a			Test 1b		
	$\alpha(^{\circ})$	$\delta(^{\circ})$	$R_d(\Omega)$	$\alpha(^{\circ})$	$\delta(^{\circ})$	$R_d(\Omega)$
0	66.850	136.690	24.349	66.850	136.690	24.349
1	60.572	131.683	23.359	55.886	133.732	22.954
2	60.723	131.757	23.124	58.139	133.425	22.892
3	60.715	131.761	23.122	58.291	133.337	22.924
4	60.715	131.761	23.122	58.293	133.336	22.925
5	60.715	131.761	23.122	58.293	133.336	22.925

TABLE 2. DC harmonic voltages for Test 1.

k	Test 1a		k	Test 1b	
	$\tilde{U}_{dk}(V)$	$\theta_{dk}(^{\circ})$		$\tilde{U}_{dk}(V)$	$\theta_{dk}(^{\circ})$
0	152.06	90.000	0	151.410	90.000
2	4.1511	157.457	2	4.0838	157.655
4	1.3812	-48.188	4	1.2621	-48.463
6	0.4149	99.774	6	0.3137	94.480
8	0.0791	-155.596	8	0.0769	160.841
10	0.0654	-82.395	10	0.0728	-92.442

TABLE 3. AC harmonic currents for Test 1.

k	Test 1a		k	Test 1b	
	$\hat{I}_k(A)$	$\phi_k(^{\circ})$		$\hat{I}_k(A)$	$\phi_k(^{\circ})$
1	12.746	-11.625	1	12.736	-11.502
3	9.8233	144.352	3	9.3940	144.469
5	5.5021	-63.060	5	4.6780	-64.552
7	1.8468	74.138	7	1.2040	54.335
9	0.7986	135.806	9	1.0459	114.997
11	0.8339	-109.783	11	0.7707	-119.928

that the converter solution is a full Newton solution and therefore a very good convergence is achieved. Once the converter solution is reached, the results corresponding to the dc harmonic voltages and the ac harmonic currents are depicted in Tables 2 and 3. These results are validated via time domain simulations by means of program PSCAD/EMTDC, as shown in Table 4, indicating an excellent agreement with the results provided by the reference model in Table 3. It is important to note that the reference model has been validated with measurements in [6]. Terms of the HCAM are depicted in Tables 5 and 6. It is evident that the distortion introduced in test 1b for the terminal ac voltage modifies the basic angles α and δ , the ac harmonic currents and the terms of the HCAM.

TABLE 4. AC harmonic currents from PSCAD/EMTDC for Test 1.

k	Test 1a		k	Test 1b	
	$\hat{I}_k(A)$	$\phi_k(^{\circ})$		$\hat{I}_k(A)$	$\phi_k(^{\circ})$
1	12.746	-11.625	1	12.736	-11.502
3	9.8234	144.352	3	9.3940	144.469
5	5.5021	-63.060	5	4.6780	-64.552
7	1.8468	74.137	7	1.2040	54.335
9	0.7986	135.805	9	1.0459	114.998
11	0.8339	-109.783	11	0.7707	-119.928

VII. TEST 2 FOR THE ITERATIVE HARMONIC ANALYSIS

This test is based on test 1a, in which the impedance $0,4 + j0,25 \Omega$ is split into two impedances: an internal impedance

TABLE 5. Terms of the HCAM (+) for Test 1.

		Test 1a		Test 1b	
k	m	G_{km}^{+}	B_{km}^{+}	G_{km}^{+}	B_{km}^{+}
1	1	0.07356	-0.01513	0.09097	-0.01831
1	5	0.79762	-0.15369	0.87121	-0.16705
5	1	0.01469	-0.02890	0.01635	-0.03185
5	5	0.21795	-0.33561	0.22519	-0.34817

TABLE 6. Terms of the HCAM (-) for Test 1.

		Test 1a		Test 1b	
k	m	G_{km}^{-}	B_{km}^{-}	G_{km}^{-}	B_{km}^{-}
1	1	0.14654	-0.37105	0.16596	-0.41416
1	5	0.23639	-0.37850	0.22421	-0.24973
5	1	0.14972	0.10451	0.14275	0.11982
5	5	0.29933	0.29238	0.26404	0.32369

$R_g + jX_g$ of the AC network and an internal impedance $R + jX$ of the power electronic rectifier. The internal voltage of the AC network only presents fundamental component and it is given by: $\hat{E}_{g1} = 120\sqrt{2} \cdot \exp(j0)$. Three cases have been considered as shown in Table 7 in which $R_g + R = 0.4 \Omega$ and $X_g + X = 0.25 \Omega$. The terminal harmonic voltages \hat{E}_k are the unknowns in the ac network solution and the initial values for these magnitudes are: $\hat{E}_1 = 120\sqrt{2} \cdot \exp(j0)$ and $\hat{E}_k = 0$ for $k \neq 1$. The converter solutions are performed with a relative tolerance of $\epsilon_I = 0.001\%$ for terms α , δ and G_d , while the ac network solution is carried out with a tolerance of $\epsilon_{II} = 10^{-5}$ pu for the harmonic voltages \hat{E}_k with respect to a base of $120\sqrt{2}$ V.

TABLE 7. Convergence properties for Test 2.

Test	R_g	X_g	R	X	Iter (DNS)	Iter (GA)
2a	0.20	0.05	0.20	0.20	6	8
2b	0.25	0.10	0.15	0.15	7	NC
2c	0.30	0.10	0.10	0.15	8	NC

TABLE 8. Evolution of the fifth harmonic voltage for Test 2.

Iter	Test 2b		Test 2c	
	$\hat{E}_5(V)$ (DNS)	$\hat{E}_5(V)$ (GA)	$\hat{E}_5(V)$ (DNS)	$\hat{E}_5(V)$ (GA)
1	2.255	3.907	2.197	4.117
2	2.798	2.358	2.828	2.376
3	3.014	3.674	3.094	3.882
4	3.062	2.590	3.176	2.778
5	3.073	3.459	3.199	3.585
6	3.075	2.772	3.206	3.175
7	3.075	3.309	3.207	3.335
8	3.076	2.900	3.208	3.460

The number of iterations for the ac network solution is indicated in Table 7 when the first 25 ac odd harmonics are considered. The modular decoupled Newton solution (M-DNS) presents very good convergence in the three cases while the Gauss Algorithm (GA) does not converge in test 2b and test 2c due to the existence of weak ac networks. By inspection of Table 8, the magnitude \hat{E}_5 of voltage \hat{E}_5

TABLE 9. AC harmonic currents for Test 2.

	Test 2a	Test 2b	Test 2c
k	$\hat{I}_k(A)$	$\hat{I}_k(A)$	$\hat{I}_k(A)$
1	12.746	12.746	12.746
3	9.8232	9.8233	9.8233
5	5.5018	5.5018	5.5019
7	1.8466	1.8464	1.8465
9	0.7987	0.7989	0.7989
11	0.8337	0.8337	0.8337

presents an oscillatory behaviour in test 2b and in test 2c during the iterative process when the GA is used. However, the evolution of \hat{E}_5 converges without problem to the solution when the M-DNS is selected. Finally, the resulting ac harmonic currents are shown in 9 for tests 2a, 2b, and 2c. The comparison of tables 3 and 9 indicates that the truncation effect is very low.

VIII. CONCLUSION

The reference model of the single-phase uncontrolled rectifier (SPUR) with finite capacitive dc smoothing has been formulated by means of a DAP based on the analytical solution of differential equations. A merit figure has been proposed to define the operating point of the converter in terms of power so that the converter solution is carried out by a full Newton method in which the terms of the Jacobian matrix present analytical expressions and the switching instants and the dc resistance are simultaneously updated. The harmonic currents of the ac side and of the dc side can be evaluated through the same compact formula by selecting the corresponding harmonic orders.

The harmonically coupled admittance matrix (HCAM) of the reference model presents a clear complexity. However, it is shown in this paper that the elimination of the phasor, associated with the transient component of the conduction interval, provides a relative easy way to obtain analytical expressions for the terms of the HCAM. The HCAM is the core of the M-DNS. The iterative harmonic analysis (IHA) presents very good convergence properties when the M-DNS is used in the three proposed experiments. However, the Gauss algorithm fails to converge in two experiments. Therefore, the proposed HCAM provides a clear improvement in the IHA with SPURs.

APPENDIX A DETAILS OF THE CONVERTER SOLUTION

The initial conditions $u_d(\alpha)$ and $u'_d(\alpha)$ must be calculated for subinterval s_x . Since $i_d(\alpha) = i'_d(\alpha) = 0$, the inspection of (7) leads to the first condition:

$$u_d(\alpha) = e(\alpha) \tag{57}$$

Since $i_d(\alpha) = 0$, the inspection of (8) and (57) leads to the second condition:

$$u'_d(\alpha) = -\sigma \cdot e(\alpha) \tag{58}$$

Voltage u_d in subinterval s_y is expressed by:

$$u_d(\tau) = u_d(\delta) \cdot \varepsilon^{-\sigma(\tau-\delta)} \quad \text{for } \tau \in s_y \quad (59)$$

where σ is defined in (8). Therefore, the final angle of subinterval s_y is given by:

$$u_d(\alpha + \pi) = u_d(\delta) \cdot \varepsilon^{-\sigma(\alpha+\pi-\delta)} \quad (60)$$

Since $u_d(\alpha + \pi) = u_d(\alpha) = e(\alpha)$, term $u_d(\delta)$ of (60) can be expressed by:

$$u_d(\delta) = e(\alpha) \cdot \varepsilon^{\sigma(\alpha+\pi-\delta)} \quad (61)$$

From (6), (8) and (61), term $u'_d(\delta_p)$ can be written as:

$$u'_d(\delta) = -\sigma \cdot e(\alpha) \cdot \varepsilon^{\sigma(\alpha+\pi-\delta)} \quad (62)$$

Finally, the combination of (59) and (61) leads to the expression for voltage $u_d(\tau)$ in discontinuity subinterval s_y :

$$u_d(\tau) = e(\alpha) \cdot \varepsilon^{\sigma(\alpha+\pi-\tau)} \quad \text{for } \tau \in s_y \quad (63)$$

Expression (63) completely describes voltage $u_d(\tau)$ during discontinuity subinterval s_y .

The main object of the converter solution is to determine basic angles α and δ . To do that, four basic equations must be considered for interval s . They are obtained from the conditions indicated in (57), (58), (61) and (62). Taking into account (11) to (16), these conditions can be written as:

$$a_1 = e(\alpha) - u_s(\alpha) = u_t(\alpha) \quad (64)$$

$$a_2 = -\sigma e(\alpha) - u'_s(\alpha) = u'_t(\alpha) \quad (65)$$

$$a_3 = e(\alpha) \cdot \varepsilon^{\sigma(\alpha+\pi-\delta)} - u_s(\delta) = u_t(\delta) \quad (66)$$

$$a_4 = -\sigma \cdot e(\alpha) \cdot \varepsilon^{\sigma(\alpha+\pi-\delta)} - u'_s(\delta) = u'_t(\delta) \quad (67)$$

Functions a_1 to a_4 present a first equivalence with the steady state component u_s and voltage e . This first equivalence can be expressed in more detail by:

$$a_1 = \sum_{m=1}^{n_h} \text{Im} \left\{ (1 - \underline{c}_m) \cdot \hat{\underline{E}}_m \cdot \varepsilon^{jm\alpha} \right\} \quad (68)$$

$$a_2 = - \sum_{m=1}^{n_h} \text{Im} \left\{ (\sigma + jm\underline{c}_m) \cdot \hat{\underline{E}}_m \cdot \varepsilon^{jm\alpha} \right\} \quad (69)$$

$$a_3 = \sum_{m=1}^{n_h} \text{Im} \left\{ \begin{array}{l} \hat{\underline{E}}_m \cdot \varepsilon^{\sigma(\alpha+\pi-\delta)} \cdot \varepsilon^{jm\alpha} \\ - \underline{c}_m \hat{\underline{E}}_m \cdot \varepsilon^{jm\delta} \end{array} \right\} \quad (70)$$

$$a_4 = - \sum_{m=1}^{n_h} \text{Im} \left\{ \begin{array}{l} \sigma \hat{\underline{E}}_m \cdot \varepsilon^{\sigma(\alpha+\pi-\delta)} \cdot \varepsilon^{jm\alpha} \\ + jm\underline{c}_m \hat{\underline{E}}_m \cdot \varepsilon^{jm\delta} \end{array} \right\} \quad (71)$$

Functions a_3 and a_4 depend on basic angles α and δ as shown in (70) and (71), while functions a_1 and a_2 only depend on basic angle α as shown in (68) and (69).

Functions a_1 to a_4 of (64) to (67) present a second equivalence with the transient component u_t and its derivative u'_t . In accordance with (14) and (16), terms u_t and u'_t depend on phasor $\hat{\underline{U}}_t$. However, phasor $\hat{\underline{U}}_t$ of voltage u_t is not known in advance. A key aspect of the analysis is the process by which phasor $\hat{\underline{U}}_t$ is expressed as a combination of functions

a_1 and a_2 , whose form is indicated in (68) and (69). To do that, auxiliary angle γ , and auxiliary phasors \underline{V} and $\underline{\lambda}$ are defined by:

$$\gamma = \delta - \alpha; \quad \underline{V} = \hat{\underline{U}}_t \cdot \varepsilon^{j\gamma}; \quad \underline{\lambda} = \varepsilon^{j\gamma} \quad (72)$$

Taking into account (14), (16 and (76), voltages $u_t(\alpha)$ and $u_t(\delta)$, and their derivatives, are equivalent to:

$$u_t(\alpha) = \text{Im}\{\underline{V}\}; \quad u_t(\delta) = \text{Im}\{\underline{V} \cdot \underline{\lambda}\} \quad (73)$$

$$u'_t(\alpha) = \text{Im}\{j \cdot \underline{V}\}; \quad u'_t(\delta) = \text{Im}\{j \cdot \underline{V} \cdot \underline{\lambda}\} \quad (74)$$

Hence, (64) and (65) can be expressed by:

$$a_1 = \text{Im}\{\underline{V}\} = \frac{1}{j2} (\underline{V} - \underline{V}^*) \quad (75)$$

$$a_2 = \text{Im}\{j \cdot \underline{V}\} = \frac{1}{j2} (j \cdot \underline{V} - j \cdot \underline{V}^*) \quad (76)$$

where \underline{V} and \underline{V}^* are the unknowns of this system of two equations, whose solution is:

$$\underline{V} = \underline{a}_{12} = \frac{1}{k_n} (a_2 - j \cdot a_1) \quad (77)$$

Phasor \underline{V} is equivalent to a complex function \underline{a}_{12} , obtained as combination of functions a_1 and a_2 . Therefore, complex function \underline{a}_{12} depends only on angle α . Taking into account (66), (67), (73), (74) and (77), functions a_3 and a_4 can be written as:

$$a_3 = \text{Im}\{\underline{a}_{12} \cdot \underline{\lambda}\}; \quad a_4 = \text{Im}\{j \cdot \underline{a}_{12} \cdot \underline{\lambda}\} \quad (78)$$

It is evident that phasor $\hat{\underline{U}}_t$ has been explicitly eliminated in both relations of (78) if functions a_3 , a_4 and \underline{a}_{12} are evaluated from (68) to (71) and (77). The relations of (78) lead to the following nonlinear equations:

$$\Delta F_a = a_3 - \text{Im}\{\underline{a}_{12} \cdot \underline{\lambda}\} = 0 \quad (79)$$

$$\Delta F_b = a_4 - \text{Im}\{j \cdot \underline{a}_{12} \cdot \underline{\lambda}\} = 0 \quad (80)$$

A system of 2 mismatch equations or residues, based on (79) and (80), is built, where basic angles α and δ are treated as variables or unknowns. The Newton method is used, whose form can be written as:

$$\begin{bmatrix} \Delta F_a \\ \Delta F_b \end{bmatrix} = - \begin{bmatrix} \frac{\partial \Delta F_a}{\partial \alpha} & \frac{\partial \Delta F_a}{\partial \delta} \\ \frac{\partial \Delta F_b}{\partial \alpha} & \frac{\partial \Delta F_b}{\partial \delta} \end{bmatrix} \begin{bmatrix} \Delta \alpha \\ \Delta \delta \end{bmatrix} \quad (81)$$

The initial values for basic angles α and δ are obtained from the ideal behaviour of the converter [14]: balanced and sinusoidal ac voltages and infinite capacitive dc smoothing. The analytical expressions for the terms of the Jacobian matrix are relatively simple due to the compact form of this procedure. According to (72), the derivatives of term $\underline{\lambda}$ are given by:

$$\frac{\partial \underline{\lambda}}{\partial \alpha} = - \frac{\partial \underline{\lambda}}{\partial \delta} = -j \cdot \underline{\lambda}$$

Functions a_1, a_2 and a_{12} only depend on angle α , and they are defined in (68), (69) and (77). Hence, the corresponding derivatives are:

$$\begin{aligned} \frac{\partial a_1}{\partial \alpha} &= \sum_{m=1}^{n_h} \text{Im} \left\{ jm \cdot (1 - c_m) \cdot \hat{E}_m \cdot \varepsilon^{jm\alpha} \right\} \\ \frac{\partial a_2}{\partial \alpha} &= - \sum_{m=1}^{n_h} \text{Im} \left\{ jm \cdot (\sigma + jm \cdot c_m) \cdot \hat{E}_m \cdot \varepsilon^{jm\alpha} \right\} \\ \frac{\partial a_{12}}{\partial \alpha} &= \frac{1}{k_n} \left(\frac{\partial a_2}{\partial \alpha} - v^* \frac{\partial a_1}{\partial \alpha} \right) \end{aligned}$$

Functions a_3 and a_4 only depend on angles α and δ , and they are defined in (70) and (71). Hence, the corresponding derivatives are:

$$\begin{aligned} \frac{\partial a_3}{\partial \alpha} &= \sum_{m=1}^{n_h} \text{Im} \left\{ (\sigma + jm) \hat{E}_m \cdot \varepsilon^{\sigma(\alpha+\pi-\delta)} \cdot \varepsilon^{jm\alpha} \right\} \\ \frac{\partial a_4}{\partial \alpha} &= - \sum_{m=1}^{n_h} \text{Im} \left\{ \sigma(\sigma + jm) \hat{E}_m \cdot \varepsilon^{\sigma(\alpha+\pi-\delta)} \cdot \varepsilon^{jm\alpha} \right\} \\ \frac{\partial a_3}{\partial \delta} &= - \sum_{m=1}^{n_h} \text{Im} \left\{ \begin{array}{l} \sigma \hat{E}_m \cdot \varepsilon^{\sigma(\alpha+\pi-\delta)} \cdot \varepsilon^{jm\alpha} \\ + jm c_m \hat{E}_m \cdot \varepsilon^{jm\delta} \end{array} \right\} \\ \frac{\partial a_4}{\partial \delta} &= \sum_{m=1}^{n_h} \text{Im} \left\{ \begin{array}{l} \sigma^2 \hat{E}_m \cdot \varepsilon^{\sigma(\alpha+\pi-\delta)} \cdot \varepsilon^{jm\alpha} \\ + m^2 c_m \hat{E}_m \cdot \varepsilon^{jm\delta} \end{array} \right\} \end{aligned}$$

Residues ΔF_a and ΔF_b depend on angles α and δ , and they are defined in (79) and (80). Hence, the corresponding terms of the Jacobian matrix present the following expressions:

$$\begin{aligned} \frac{\partial \Delta F_a}{\partial \alpha} &= \frac{\partial a_3}{\partial \alpha} - \text{Im} \left\{ \frac{\partial a_{12}}{\partial \alpha} \lambda + a_{12} \frac{\partial \lambda}{\partial \alpha} \right\} \\ \frac{\partial \Delta F_b}{\partial \alpha} &= \frac{\partial a_4}{\partial \alpha} - \text{Im} \left\{ v \frac{\partial a_{12}}{\partial \alpha} \lambda + v \cdot a_{12} \frac{\partial \lambda}{\partial \alpha} \right\} \\ \frac{\partial \Delta F_a}{\partial \delta} &= \frac{\partial a_3}{\partial \delta} - \text{Im} \left\{ a_{12} \cdot \frac{\partial \lambda}{\partial \delta} \right\} \\ \frac{\partial \Delta F_b}{\partial \delta} &= \frac{\partial a_4}{\partial \delta} - \text{Im} \left\{ v \cdot a_{12} \cdot \frac{\partial \lambda}{\partial \delta} \right\} \end{aligned}$$

We can observe that the terms of the Jacobian matrix present simple analytical expressions.

APPENDIX B HARMONIC CURRENTS

In accordance with (8) and (11), current $i_d(\tau)$ can be obtained from voltage $u_d(\tau)$, and this voltage can be expressed in function of components u_t and u_s . Hence, current i_d can also be split into two components i_t and i_s , so that:

$$i_d = i_t + i_s; \quad \begin{cases} i_t = G_d \cdot u_t + B_c \cdot u'_t \\ i_s = G_d \cdot u_s + B_c \cdot u'_s \end{cases}$$

Taking into account (21) and (22), components i_t and i_s can be written as:

$$i_t(\tau) = \frac{1}{j2} (d_t \cdot \hat{U}_t \varepsilon^{j\tau} - d_t^* \cdot \hat{U}_t^* \varepsilon^{j^* \tau}) \quad (82)$$

$$\begin{aligned} i_s(\tau) &= \frac{1}{j2} \sum_{m=1}^{n_h} (d_m \cdot \hat{E}_m \varepsilon^{jm\tau} - d_m^* \cdot \hat{E}_m^* \varepsilon^{-jm\tau}) \\ d_t &= G_d + v B_c \quad d_m = c_m (G_d + jm \cdot B_c) \quad (83) \end{aligned}$$

In accordance with (23), the harmonic contributions of terms i_t and i_s are defined as $F_{k,t}$ and $F_{k,s}$ respectively, and they are obtained from:

$$F_{k,t} = F_k(i_t); \quad F_{k,s} = F_k(i_s)$$

Taking into account (82) and (83), the harmonic contributions $F_{k,t}$ and $F_{k,s}$ present the following compact form:

$$\begin{aligned} F_{k,t} &= \beta_{k,t}^{(1)} \cdot d_t \cdot \hat{U}_t + \beta_{k,t}^{(2)} \cdot d_t^* \cdot \hat{U}_t^* \\ F_{k,s} &= \sum_{m=1}^{n_h} (\beta_{km,s}^{(1)} \cdot d_m \cdot \hat{E}_m + \beta_{km,s}^{(2)} \cdot d_m^* \cdot \hat{E}_m^*) \end{aligned}$$

where terms β are indicated in (26) to (30). Therefore, function F_k is equivalent to:

$$F_k = F_{k,t} + F_{k,s}$$

APPENDIX C DERIVATIVES $\partial \Delta F_a / \partial G_d$ AND $\partial \Delta F_b / \partial G_d$

Derivatives with respect to G_d are denoted by subscript g . Hence, we have:

$$\sigma_g = 2\xi_g = \frac{1}{B_c}; \quad k_{0g} = \frac{R}{2k_0 X B_c} \quad (84)$$

$$k_{ng} = \frac{k_0 k_{0g} - \xi \xi_g}{k_0}; \quad c_{mg} = -(R + jmX) c_m^2 \quad (85)$$

$$v_g = -\xi_g + jk_{ng}; \quad \lambda_g = \gamma \cdot \lambda \cdot v_g \quad (86)$$

Therefore, the derivatives of a_1, a_2, a_3, a_4 and a_{12} are:

$$a_{1g} = - \sum_{m=1}^{n_h} \text{Im} \left\{ c_{mg} \cdot \hat{E}_m \cdot \varepsilon^{jm\alpha} \right\} \quad (87)$$

$$a_{2g} = - \sum_{m=1}^{n_h} \text{Im} \left\{ (\sigma_g + jm c_{mg}) \cdot \hat{E}_m \cdot \varepsilon^{jm\alpha} \right\} \quad (88)$$

$$a_{3g} = \sum_{m=1}^{n_h} \text{Im} \left\{ \begin{array}{l} (\pi - \gamma) \sigma_g \hat{E}_m \cdot \varepsilon^{\sigma(\pi-\gamma)} \cdot \varepsilon^{jm\alpha} \\ - c_{mg} \hat{E}_m \cdot \varepsilon^{jm\delta} \end{array} \right\} \quad (89)$$

$$a_{4g} = - \sum_{m=1}^{n_h} \text{Im} \left\{ \begin{array}{l} [1 + \sigma(\pi - \gamma)] \sigma_g \hat{E}_m \cdot \varepsilon^{\sigma(\pi-\gamma)} \cdot \varepsilon^{jm\alpha} \\ + jm c_{mg} \hat{E}_m \cdot \varepsilon^{jm\delta} \end{array} \right\} \quad (90)$$

$$a_{12g} = \frac{1}{k_n} (a_{2g} - v_g^* a_{1g} - v^* a_{1g} - k_{ng} a_{12}) \quad (91)$$

With this, derivatives $\partial \Delta F_a / \partial G_d$ and $\partial \Delta F_b / \partial G_d$ are:

$$\frac{\partial \Delta F_a}{\partial G_d} = a_{3g} - \text{Im} \{ a_{12g} \cdot \lambda + a_{12} \cdot \lambda_g \} \quad (92)$$

$$\frac{\partial \Delta F_b}{\partial G_d} = a_{4g} - \text{Im} \{ v_g \cdot a_{12} \cdot \lambda + v \cdot a_{12g} \cdot \lambda + v \cdot a_{12} \cdot \lambda_g \} \quad (93)$$

REFERENCES

- [1] A. Mansoor, W. M. Grady, A. H. Chowdhury, and M. J. Samotyj, "An investigation of harmonics attenuation and diversity among distributed single-phase power electronic loads," *IEEE Trans. Power Del.*, vol. 10, no. 1, pp. 467–473, Jan. 1995.
- [2] A. Mansoor, W. M. Grady, R. S. Thallam, M. T. Doyle, S. D. Krein, and M. J. Samotyj, "Effect of supply voltage harmonics on the input current of single-phase diode bridge rectifier loads," *IEEE Trans. Power Del.*, vol. 10, no. 3, pp. 1416–1422, Jul. 1995.
- [3] A. Mansoor, W. M. Grady, P. T. Staats, R. S. Thallam, M. T. Doyle, and M. J. Samotyj, "Predicting the net harmonic currents produced by large numbers of distributed single-phase computer loads," *IEEE Trans. Power Del.*, vol. 10, no. 4, pp. 2001–2006, Oct. 1995.
- [4] G. Carpinelli, F. Iacovone, P. Varilone, and P. Verde, "Single phase voltage source converters: Analytical modelling for harmonic analysis in continuous and discontinuous current conditions," *Int. J. Power Energy Syst.*, vol. 23, no. 1, pp. 37–48, 2003.
- [5] K. Lian and P. Lehn, "Harmonic analysis of single-phase full bridge rectifiers based on fast time domain method," in *Proc. IEEE Int. Symp. Ind. Electron.*, Montreal, QC, Canada, Jul. 2006, pp. 2608–2613.
- [6] J. J. Mesas, L. Sainz, and J. Molina, "Parameter estimation procedure for models of single-phase uncontrolled rectifiers," *IEEE Trans. Power Del.*, vol. 26, no. 3, pp. 1911–1919, Jul. 2011.
- [7] J. G. Mayordomo, A. Carbonero, L. F. Beites, and W. Xu, "Decoupled Newton algorithms in the harmonic domain for the harmonic interaction of line commutated converters with AC systems," *IEEE Trans. Power Del.*, vol. 25, no. 3, pp. 1721–1733, Jul. 2010.
- [8] J. G. Mayordomo, L. F. Beites, R. Asensi, F. Orzáez, M. Izzeddine, and L. Zabala, "A contribution for modeling controlled and uncontrolled AC/DC converters in harmonic power flows," *IEEE Trans. Power Del.*, vol. 13, no. 4, pp. 1501–1508, Oct. 1998.
- [9] Y. Sun, G. Zhang, W. Xu, and J. G. Mayordomo, "A harmonically coupled admittance matrix model for AC/DC converters," *IEEE Trans. Power Syst.*, vol. 22, no. 4, pp. 1574–1582, Nov. 2007.
- [10] J. Yong, L. Chen, A. B. Nassif, and W. Xu, "A frequency-domain harmonic model for compact fluorescent lamps," *IEEE Trans. Power Del.*, vol. 25, no. 2, pp. 1182–1189, Apr. 2010.
- [11] J. Yong, L. Chen, and S. Chen, "Modeling of home appliances for power distribution system harmonic analysis," *IEEE Trans. Power Del.*, vol. 25, no. 4, pp. 3147–3155, Oct. 2010.
- [12] J. Molina and L. Sainz, "Model of electronic ballast compact fluorescent lamps," *IEEE Trans. Power Del.*, vol. 29, no. 3, pp. 1363–1371, Jun. 2014.
- [13] J. G. Mayordomo, L. F. Beites, X. Yang, and W. Xu, "A detailed procedure for harmonic analysis of three-phase diode rectifiers under discontinuous conduction mode and nonideal conditions," *IEEE Trans. Power Del.*, vol. 33, no. 2, pp. 741–751, Apr. 2018.
- [14] J. G. Mayordomo, A. Hernández, R. Asensi, and L. F. M. B. Izzeddine, "A unified theory of uncontrolled rectifiers, discharge lamps and arc furnaces. Part 1: An analytical approach for normalized harmonic emission calculations," *Int. Conf. Harmon. Quality Power*, vol. 2, pp. 740–748, Oct. 1998.
- [15] N. Mohan, T. M. Undeland, and W. P. Robbins, *Power Electronic Converters, Applications, and Design*. Hoboken, NJ, USA: Wiley, 2003.
- [16] *EMTDC: Transient Analysis for PSCAD Power System Simulation. User Guide*, Manitoba Hydro Int., Winnipeg, MB, Canada, 2005.

LUIS F. BEITES received the Ph.D. degree from the Universidad Politecnica de Madrid, Madrid, Spain, in 1999. He is currently an Associate Professor with the Universidad Politecnica de Madrid. His research interests include electrical power quality, including harmonics and the effect of smart grids, microgrids, HVDCs, and all electronics implemented in the networks.

JULIO G. MAYORDOMO received the Dipl.-Eng. and Ph.D. degrees from the Universidad Politecnica de Madrid, Madrid, Spain. He is currently a Full Professor with the Universidad Politecnica de Madrid. His current research interest includes low-frequency disturbances.

XAVIER YANG (Senior Member, IEEE) received the Ph.D. degree from the National Polytechnic Institute of Toulouse, Toulouse, France, in 1994. He is currently a Senior Researcher in research and development with Electricite de France, EDF Lab Paris-Saclay, France. His research interests include micro grid, ac and dc power quality, electric power system modeling, and integration of renewable energy sources.

• • •